

Supplementary Information

**A green-by-design bioprocess for L-Carnosine production
integrating enzymatic synthesis with membrane separation**

Dong-Ya Yin,^{a#} Jiang Pan,^{a#} Jie Zhu,^b You-Yan Liu,^c and Jian-He Xu^{a*}

^a State Key Laboratory of Bioreactor Engineering, and ^b School of Chemistry and Molecular Engineering, East China University of Science and Technology, Shanghai 200237, P.R. China;

^cCollege of Chemistry and Chemical Engineering, Guangxi University, Nanning 530004, P.R. China.

*Corresponding author. E-mail: jianhexu@ecust.edu.cn.

#These authors (D.Y.Y., J.P.) contributed equally to this work.

Table of Contents

1. Genome mining of dipeptidases for <i>L</i> -Car synthesis	2
2. Characterization of <i>SmPepD</i>	4
3. Optimization of the synthetic reaction	6
4. Pilot reactions and preparation of <i>L</i> -Car	9
5. HPLC analysis.....	10
6. ¹ H NMR and ¹³ C NMR spectra of the product	12
7. Optical rotation of the <i>L</i> -Car produced	12
8. References	13

1. Genome mining of dipeptidases for L-Car synthesis

1.1 Candidates and primers used in this study

Table S1. Strains and primers used in this study

Candidates	Sources	aa	Primers (5'-3')
WP_012554100.1	<i>Gluconacetobacter diazotrophicus</i>	488	CGCGGATCCATGACGACGACGAACCGACGCGA CCGCTCGAGTCAGGCCGCGCCTGCCATGT
WP_024118972.1	<i>Thermus thermophilus</i>	432	CCGGAATTCGTGGACCTCACCGAGCTTTTTGCC CCGCTCGAGCTACCCCGCAAGGAGGCGGTGGAA
CDO56314.1	<i>Geotrichum candidum</i>	989	CGCGGATCCATGGCCCATTGGTTGAAGAGTCA CGTCGACTTAGGCGTCCTTCTCTTCCTCGGCA
WP_013454724.1	<i>Marivirga tractuosa</i>	459	CGCGGATCCATGATAACGAAAGAAGAAACA CCGCTCGAGTTACTTAGCTTTTTTCAGCAAAG
XP_008092217.1	<i>Colletotrichum graminicola</i>	476	CCGGAATTCATGGCTCCCCAACTTGACGGCTA CCGCTCGAGTTATACGGTGGGCTCCTCAGCAA
XP_011272278.1	<i>Wickerhamomyces ciferrii</i>	478	CGCGGATCCATGGCGTTCAACAAATCA CCGCTCGAGTTATTTCTCACCTTGAGCA
XP_002618402.1	<i>Clavispora lusitaniae</i>	481	CCGGAATTCATGTCGTTGATAAACTCCCCT CCGCTCGAGTTAAGCCTTACCGTAGTAGTG
XP_001824398.1	<i>Aspergillus oryzae</i>	478	CGCGGATCCATGGCACCACAGCTGGAACCA CGTCGACCTATGCCGCCACCATGGGCTCTT
XP_001643237.1	<i>Vanderwaltozyma polyspora</i>	509	CGCGGATCCATGTTGTTCAAATTGTTTTTCAAGAG CCGCTCGAGTCAGTTTTTCTGGGGATTTCAGCATA
XP_001550857.2	<i>Botrytis cinerea</i>	478	CGCGGATCCATGGCTCCTCAACTCGATGGCTA

			CCGCTCGAGTTATTGCTCAACCATTGGTTCCTC
ANZ73647.1	<i>Komagataella pastoris</i>	478	CGCGGATCCATGTCAATTGAAAAGAACTCCA CCGCTCGAGTTATATCTCACCATAGTAGTGTA
WP_012871483.1	<i>Sphaerobacter thermophilus</i>	392	CGCGGATCCGTGTCCGAATGGGAAGCCAGGCT CCGCTCGAGTCACTGCGACGGCCTCTCCCCGT
WP_061884163.1	<i>Bacillus thuringiensis</i>	489	CGCGGATCCATGTATTCTACATTAGAAC CCGCTCGAGTTACTTAGCTAATTCTTTTCG
WP_096921499.1	<i>Halomonas hydrothermalis</i>	495	CGCGGATCCATGAACGCACATCTAGAAGCGCTC CCCAAGCTTTCAGACCTGGCGACTGGCCGAGT
WP_041834588.1	<i>Actinobacillus succinogenes</i>	482	CGCGGATCCATGTCAGAAATTCAAACATTACAG CCGCTCGAGTTATTTCTCCTTAATACCGGCTAA
WP_041417794.1	<i>Shewanella woodyi</i>	486	CGCGGATCCGTGACTGCAATAAATCAATTACAA CCGCTCGAGTTATGCTTTCTCTGGAATACGTTC
XP_003870465.1	<i>Candida parapsilosis</i>	483	CGTCGACATGTCAGAGAAATACGACAAGTTACC CCGCTCGAGCTAAGCTTTAGCATAATAGTGCAA
WP_016928980.1	<i>Serratia marcescens</i>	486	CCGGAATTCGTGTCTGAATTGTCTCAGCTTT CCGCTCGAGTTACGCGCGCTCAGGGATCGCTTT
WP_012442310.1	<i>Erwinia tasmaniensis</i>	485	CGCGGATCCGTGTCTGAATTGTCTCAATTATCC CCGCTCGAGTTATTTGCGCCGGGATCGCCTTCA
WP_029739704.1	<i>Enterobacter</i>	485	CGCGGATCCGTGTCTGAACTGTCTCAATTA CCGCTCGAGTTACTTCGCAGGGATCGCTTT
WP_063108096.1	<i>Escherichia coli</i>	485	CCGGAATTCATGTCTGAACTGTCTCAATTATCTCC CCCAAGCTTCTTCGCCGGAATTTCTTTCAGCAGTT

1.2 Cloning, expression and purification of recombinant dipeptidases

The genes encoding the candidate dipeptidases were amplified by PCR reaction using the corresponding genomic DNA as template with the following primers (**Table S1**). The obtained DNA fragment was ligated into pET-28a (+) vector, and transformed into *Escherichia coli* BL21 (DE3). The recombinant *Escherichia coli* was cultured in LB medium, and induced by 0.2 mM IPTG at 16°C for 24 h. The cells obtained were disrupted by ultrasonication and the dipeptidases were purified by nickel affinity chromatography. The expression and purification of recombinant enzymes were analyzed via SDS-PAGE, as shown in **Figs. S1 - S7**.

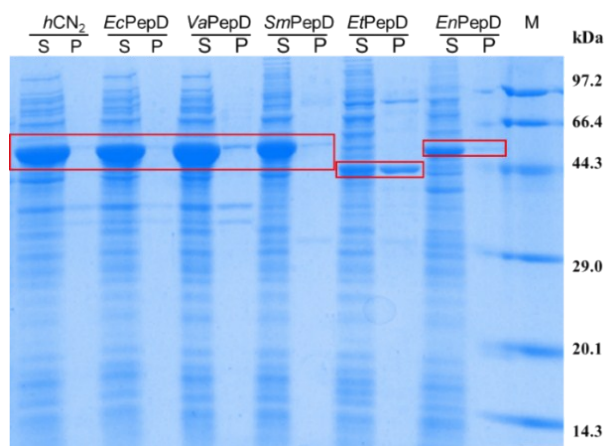


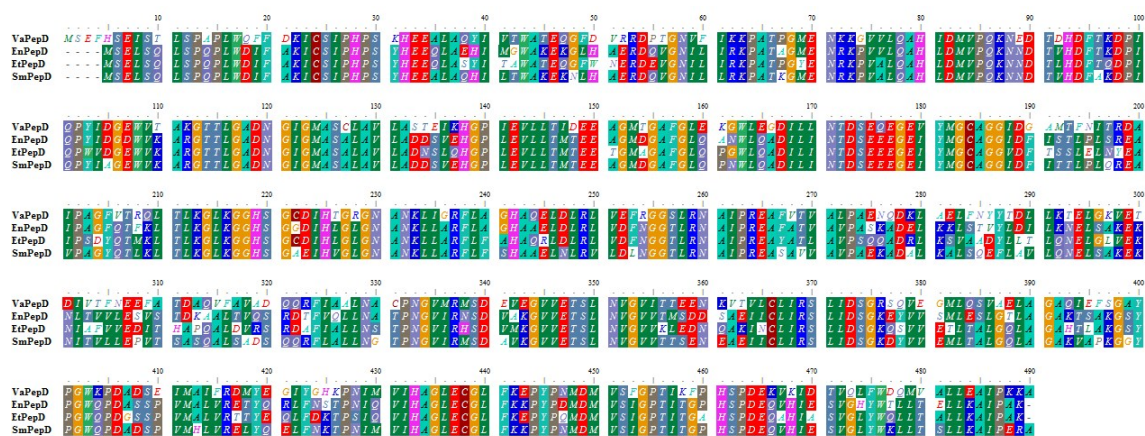
Figure S1. SDS-PAGE analysis of dipeptidases expressed in *Escherichia coli*.

M: protein marker; S: supernatant; P: precipitate.

Figures S2-S7. Purification of dipeptidases.

The dipeptidases above were *SmPepD*, *VaPepD*, *EcPepD*, *EnPepD*, *EtPepD* and *hCN2*, respectively. M: protein marker; Lane 1: supernatant of cell-free extract; Lane 2: precipitate of cell-free extract; Lane 3: solution after flowed through Ni-NTA column; Lanes 4-9: elution fractions of Ni-NTA column.

The sequence alignment diagram of *VaPepD* and every new dipeptidase was shown in the Figure S8. These new proteins share diverse identities (*EnPepD* (88%), *EtPepD* (76%), *SmPepD* (62%)) to the guide dipeptidase *VaPepD*.



Figures S8. The sequence alignment diagram of *VaPepD* and every new dipeptidase.

2. Characterization of *SmPepD*

The effects of temperature, pH, metal ions and EDTA on the *SmPepD* were characterized.

2.1 Generals

Initial synthetic activity of *SmPepD* was determined in a system of 0.2 ml buffer containing 2 M β -Ala, 100 mM *L*-His and adequate amount of purified *SmPepD*, agitated at 1,000 rpm.

2.2 Effect of temperature on the *SmPepD* activity

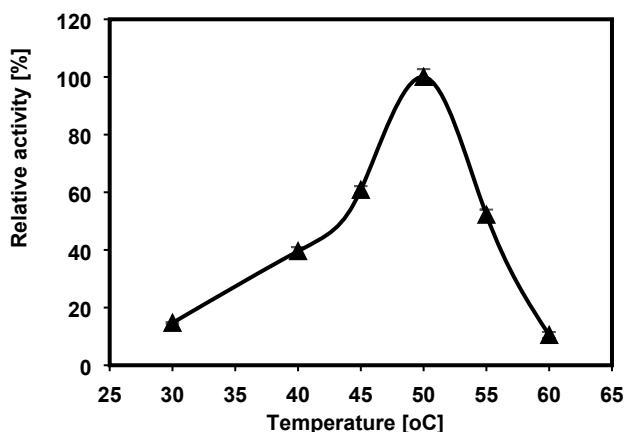


Figure S9. Effect of temperature on the activity of purified *SmPepD*. Reactions were performed at temperatures ranging from 30 to 50°C with 0.5 mg mL⁻¹ purified *SmPepD* in Tris-HCl buffer (50 mM, pH 8.0). The relative activity was expressed as a percentage of the maximum activity detected.

2.3 Effect of pH on the *SmPepD* activity

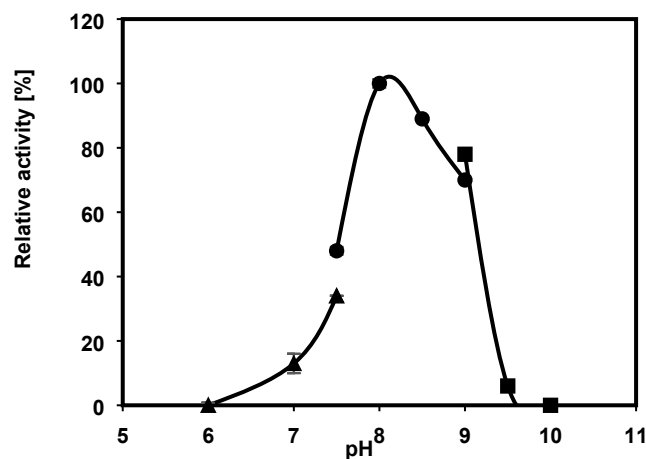


Figure S10. Effect of pH on the activity of purified *SmPepD*. For pH optimization, reactions were performed at 40°C with 0.5 mg mL⁻¹ purified *SmPepD* in system containing 50 mM buffers with various pH: (▲) phosphate potassium buffer (pH 6.0 to 7.5), (●) Tris-HCl buffer (pH 7.5 to 9.0) and (◻) Glycine-NaOH buffer (pH 9.0 to 10.0). The relative activity was expressed as a percentage of the maximum activity detected.

2.4 Thermostability of *SmPepD*

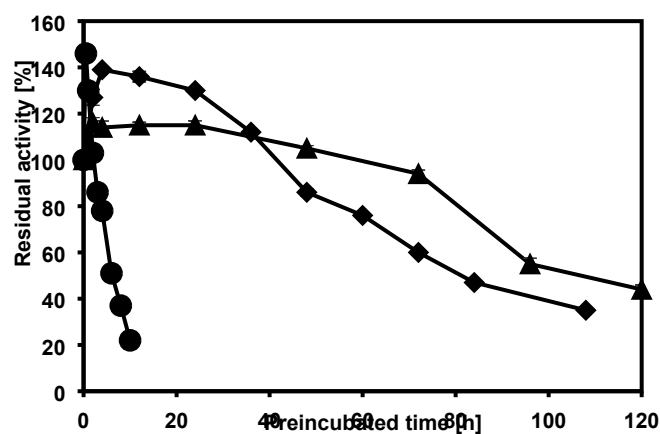


Figure S11. Effect of temperature on the stability of purified *SmPepD*. Purified *SmPepD* of 5 mg mL⁻¹ was incubated in Tris-HCl buffer (50 mM, pH 8.0) at various temperatures ranging from 30 to 50°C. Samples were withdrawn intermittently and placed on ice immediately. Then the residual synthetic activity of *SmPepD* was measured at 30°C, pH 8.0. The residual activity was expressed as a percentage of the initial activity detected. (◻) 30°C; (●) 40°C; (▲) 50°C.

2.5 Effect of Mn²⁺ concentration on the *SmPepD* activity

Table S4. Effect of Mn^{2+} concentration on the *SmPepD* activity.

Concentration of $MnCl_2$	Relative activity (%)
0	100 ± 2
0.001	144 ± 14
0.005	616 ± 3
0.01	998 ± 3
0.05	1864 ± 6
0.1	2274 ± 2
0.5	2208 ± 3
1.0	2127 ± 4

Reactions were performed at 40°C with 0.5 mg mL⁻¹ purified *SmPepD* in Tris-HCl buffer (50 mM, pH 8.0) with or without $MnCl_2$. The relative activity was expressed as a percentage of the activity detected in system without $MnCl_2$.

3. Optimization of the synthetic reaction

3.1 Preparation of lyophilized cell-free extract

Lyophilized cell-free extract was prepared for easy to store and future use. After ultrasonication (400 W, 15 minutes) and centrifugation (4°C, 13,500 × g, 35 min) of cells obtained, the cell-free extract was separated and frozen at -80°C for overnight and lyophilized for 48 h. The specific activity of the prepared lyophilized cell-free extract was determined as 150 U g⁻¹.

3.2 Reversible reaction performed in both directions

SmPepD catalyzed synthesis of *L*-Car is a reversible reaction, both hydrolysis and synthesis of *L*-Car were performed simultaneously to determine the equilibrium concentration of *L*-Car. The reactions in systems containing Tris-HCl buffer at pH 8.0, 30°C were shown in **Figure S12**.

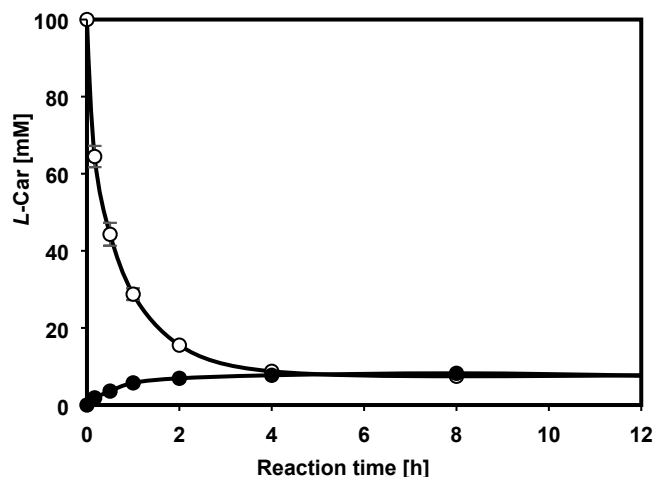


Figure S12. Process curves of both hydrolytic and synthetic reaction in system containing Tris-HCl buffer. For Synthetic reaction (●), the reaction system was composed of Tris-HCl (50 mM, pH was adjusted by NaOH solution to 8.0) containing 2.0 M β -Ala and 100 mM *L*-His; while for hydrolytic reaction (○), the reaction system was composed of Tris-HCl (50 mM, pH was adjusted by NaOH solution to 8.0) containing 1.9 M β -Ala and 100 mM *L*-Car.

3.3 Effect of buffer on synthetic activity and K_{eq}

The reactions were performed in the systems containing Tris-HCl buffer (50 mM, pH was adjusted by NaOH solution to 8.0) or pure water without buffer salt (pH was adjusted by NaOH solution to 8.0), at 30°C. The synthetic activity of *SmPepD* and equilibrium concentration of *L*-Car ($[Car]_{eq}$) in both systems were measured, and K_{eq} was calculated, as shown in **Table S5**.

Table S5. Effect of buffer on synthetic activity and K_{eq}

Medium	Synthetic activity ($\text{mmol h}^{-1} \text{g}_{\text{catalyst}}^{-1}$)	$[Car]_{eq}$ (mM)	K_{eq}
Tris-HCl buffer (50 mM, pH 8.0)	0.34 ± 0.02	7.52 ± 0.10	1.98
Pure water (pH 8.0)	0.35 ± 0.01	7.62 ± 0.04	2.01

3.4 Effect of temperature on K_{eq}

The reactions were performed at various temperatures from 30 to 50°C with pH 8.0. The

process curve of *L*-Car synthesis was shown as **Figure S13**, and the $[\text{Car}]_{\text{eq}}$ and K_{eq} were listed in **Table S6**.

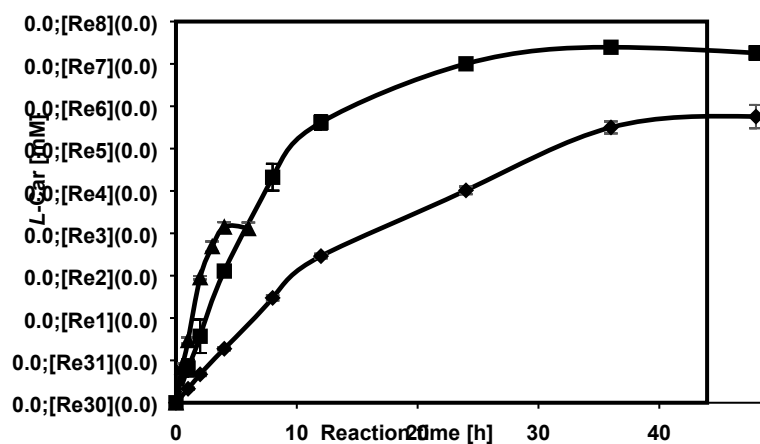


Figure S13. Process curves of *L*-Car at different temperatures. Symbols: (*) 30°C; (●) 40°C; (□) 50°C.

Table S6. Effect of temperature on the equilibrium concentration of *L*-Car.

Temperature (°C)	$[\text{Car}]_{\text{eq}}$ (mM)	K_{eq}
30	7.62 ± 0.03	2.01
40	8.48 ± 0.07	2.23
50	8.79 ± 0.04	2.37

3.5 Effect of pH on synthetic activity and K_{eq}

The reactions were performed in various initial pH at 40°C. The synthetic activity of *SmPepD* and equilibrium concentration of *L*-Car ($[\text{Car}]_{\text{eq}}$) were measured, and K_{eq} was calculated, as shown in **Table S7**.

Table S7. Effect of pH on initial synthetic rate and *L*-Car production.

Initial pH	Synthetic activity ($\text{mmol h}^{-1} \text{g}^{-1}$)	$[\text{Car}]_{\text{eq}}$ (mM)	K_{eq}
7.0	0.09 ± 0.01	10.85 ± 0.25	2.97

8.0	0.35 ± 0.02	8.48 ± 0.07	2.23
9.0	0.28 ± 0.01	7.34 ± 0.02	1.93

3.6 Process of synthetic reaction under the optimal condition

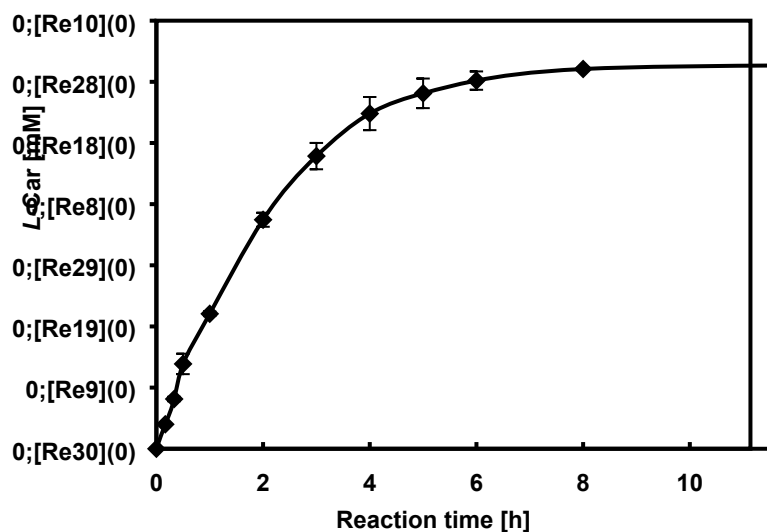
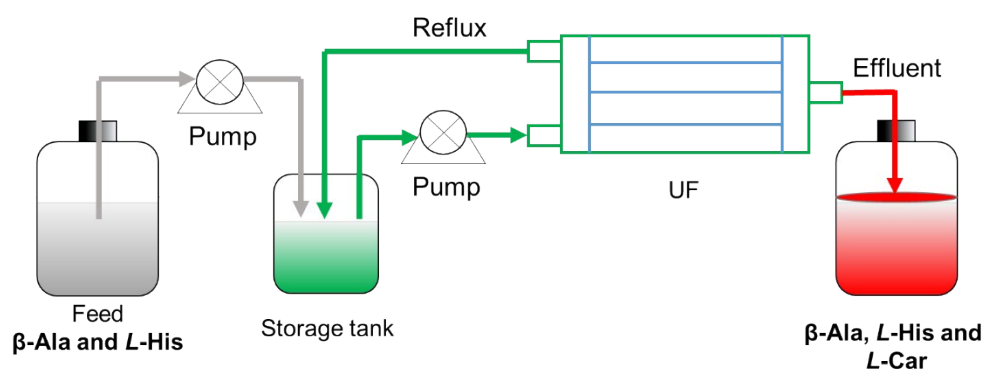


Figure S14. Time course of the 10 mL reaction of *L-Car* in the optimal condition. The reaction was performed in 10 mL system containing saturated substrates, 0.1 mM MnCl_2 , lyophilized cell-free extract of *SmPepD* (75 U L^{-1}) at pH 8.0, magnetic stirred at 600 rpm, 40°C .

4. Pilot reactions and preparation of *L-Car*

4.1 Diagram of UF-MBR



Scheme S1. Diagram of UF-MBR.

4.2 Determination of retention (*R*) by UF membrane ^[S1]

A NF membrane DK 1812 with MWCO of 150 Da was applied for separation of *L*-Car. Solution of 5 L containing 1 M β -Ala, 100 mM *L*-His and 50 mM *L*-Car was applied for the determination of apparent rejection rate. The NF process was performed at a pressure of 3 MPa with the permeate liquid returned to the storage tank for 30 min to made the system stabilization. The concentrations of each compound in permeate liquid and storage tank were measured. The *R* was calculated according to **Equation S1**. The results were shown in **Table S8**.

$$R = [S]_p / [S]_s \quad \text{Equation S1}$$

Where $[S]_p$ represent the concentrations of each compound in permeate liquid; $[S]_s$ represent the concentrations of each compound in storage tank.

Table S8. Retention (*R*) of substrates and product.

Entry	Molecular weight (D)	<i>R</i> (%)
β -Ala	89	46.5
<i>L</i> -His	155	65.7
<i>L</i> -Car	226	92.3

5. HPLC analysis

5.1 Retention times of substrates and *L*-Car

substances	retention time (min)
β -Ala	6.4
<i>L</i> -His	5.8
<i>L</i> -Car	9.8

5.2 Retention times and calibration curves of substrates and *L*-Car

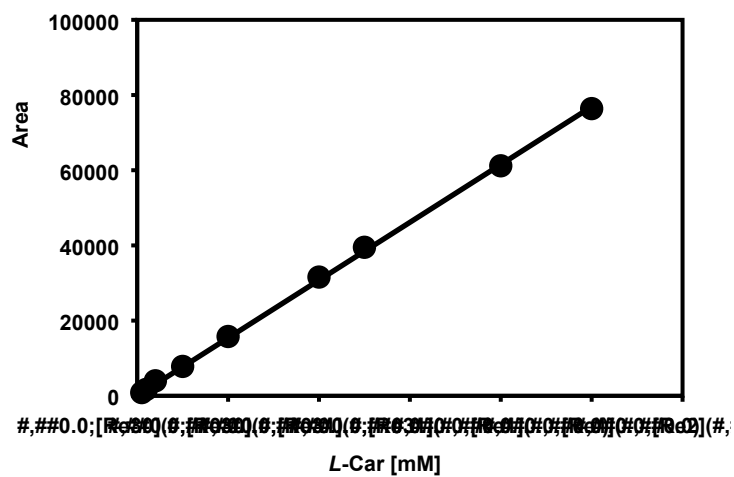
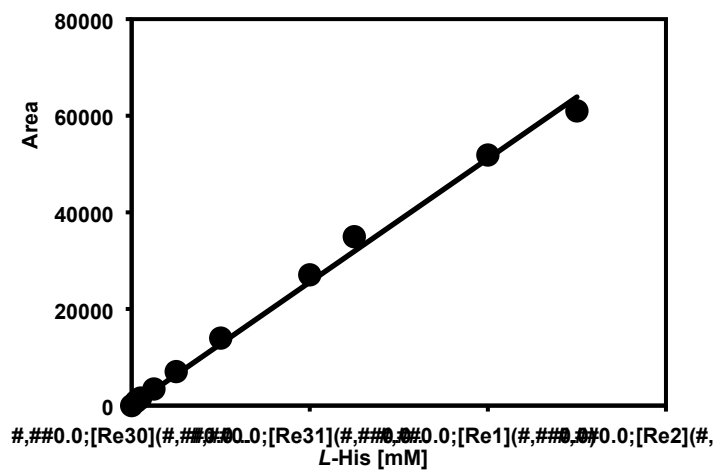
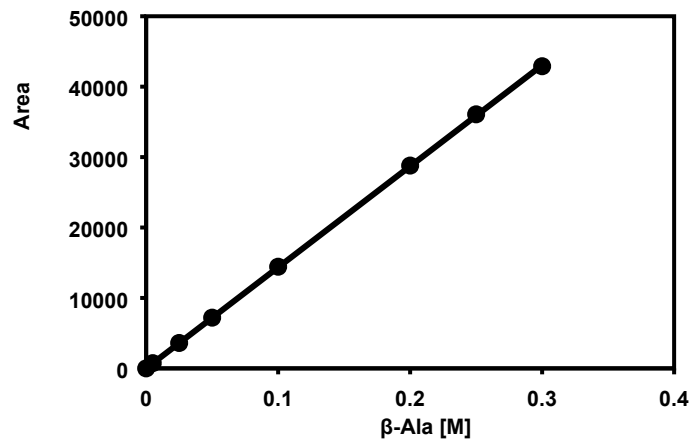


Figure S15. HPLC calibration curves of β -Ala, L-His and L-Car.

5.2 HPLC spectra before and after the NF process

HPLC spectra of the reaction mixture before NF and the refined solution after NF were shown in Figure S16.

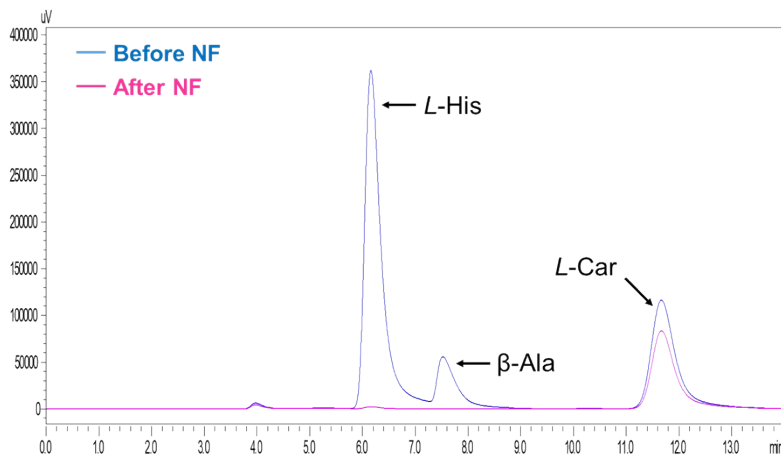
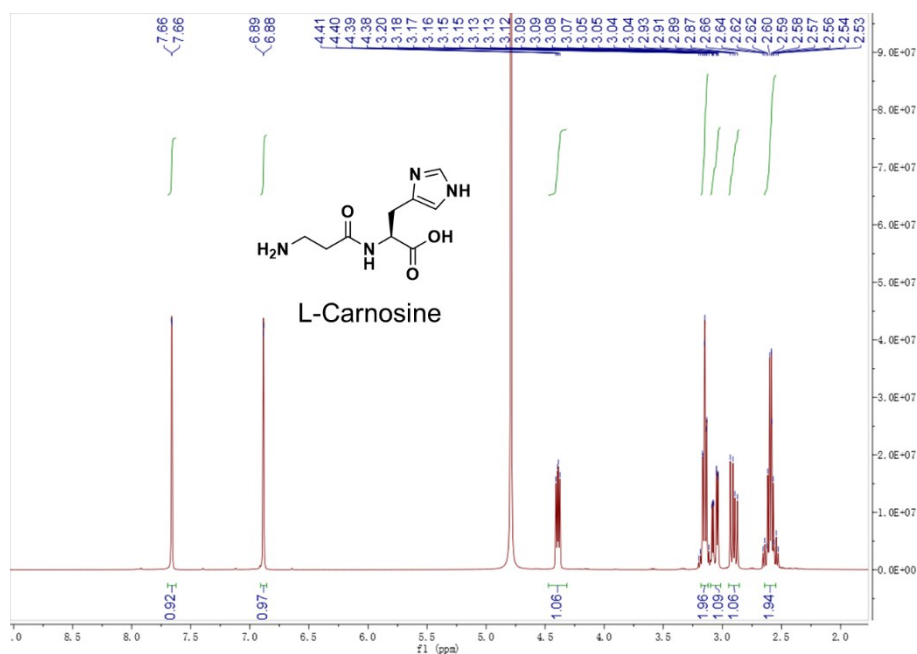
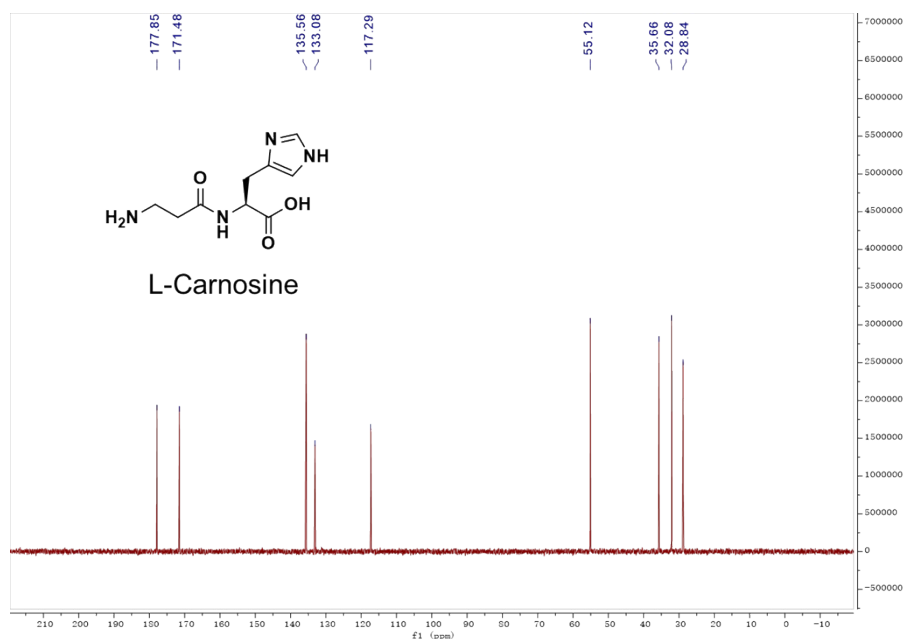


Figure S16. HPLC spectra of the reaction mixture (before NF) and refined product (after NF).

6. ^1H NMR and ^{13}C NMR spectra of the product [S2]



^1H NMR (400 MHz, D_2O) δ /ppm 7.66 (d, $J = 1.3$ Hz, 1H), 6.88 (d, $J = 1.1$ Hz, 1H), 4.39 (dd, $J = 8.7, 4.7$ Hz, 1H), 3.15 (td, $J = 6.6, 1.5$ Hz, 2H), 3.06 (ddd, $J = 15.1, 4.8, 0.8$ Hz, 1H), 2.90 (dd, $J = 15.0, 8.8$ Hz, 1H), 2.64 – 2.55 (m, 2H).



^{13}C NMR (100 MHz, D_2O) δ/ppm 177.85 , 171.48 , 135.56 , 133.08 , 117.29 , 55.12 , 35.66 , 32.08 , 28.84 .

7. Optical rotation of the *L*-Car produced

A solution of 30 mg mL^{-1} produced *L*-Car in water was prepared and put into a polarizer tube of 1 dm. The optical rotation (α) at 589 nm was determined on a spectrometer Aocptd I (Rudolph Research Analytical Co., Ltd., American) as described.^[S2] The specific rotation $[\alpha]$ was calculated using the following formula:

$$[\alpha] = \alpha / (c \cdot l)$$

Where c represents the content of *L*-Car (g mL^{-1}); l represents the length of polarizer tube (dm).

8. References

[S1] C. O. Martin, S. Bouhallab and A. Garem, *J. Membrane Sci.*, 1998, **142**(2): 225-233.

[S2] M. S. Cherevin, Z. P. Zubreichuk and L. A. Popova, *Russ. J. Gen. Chem.*, 2007, **77**: 1576-1579.